Electronic Supplementary Material (ESI) for Journal of Materials Chemistry C.

The Effect of Regioisomerism on the Crystal Packing and Device Performance of Desymmetrized Anthradithiophenes

Rawad K. Hallani[a], Karl J. Thorley[a], Anna K. Hailey[b], Sean R. Parkin[a], Yueh-Lin Loo[b], and John E. Anthony*[a]

[a]Department of Chemistry, University of Kentucky, Lexington, KY

[b]Department of Chemical Engineering, Princeton University, Princeton, NJ

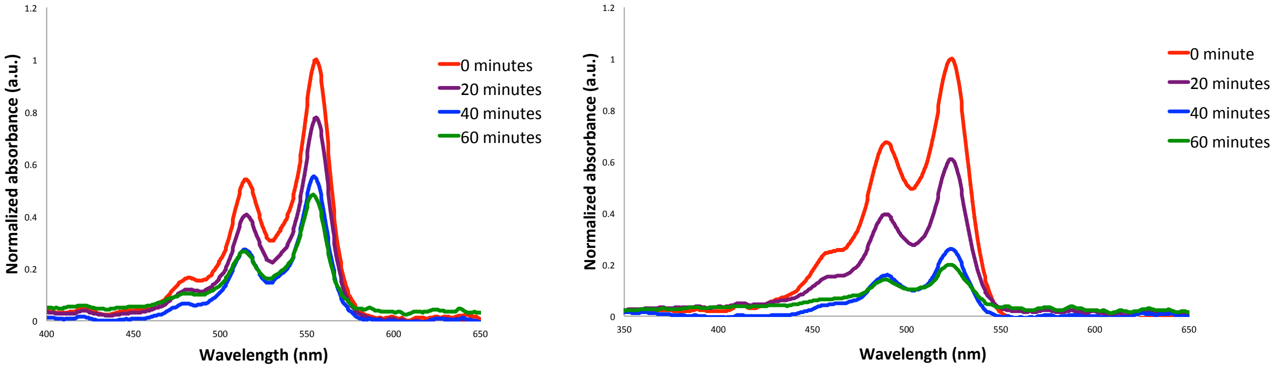

Fig. S7 Photostability measurements in dichloromethane for TSBS ADT (left) $t_{1/2}$ = 54 minutes, and the isomeric mixture of **3a, 3b,** and **3c** (right) $t_{1/2}$ = 18 minutes.

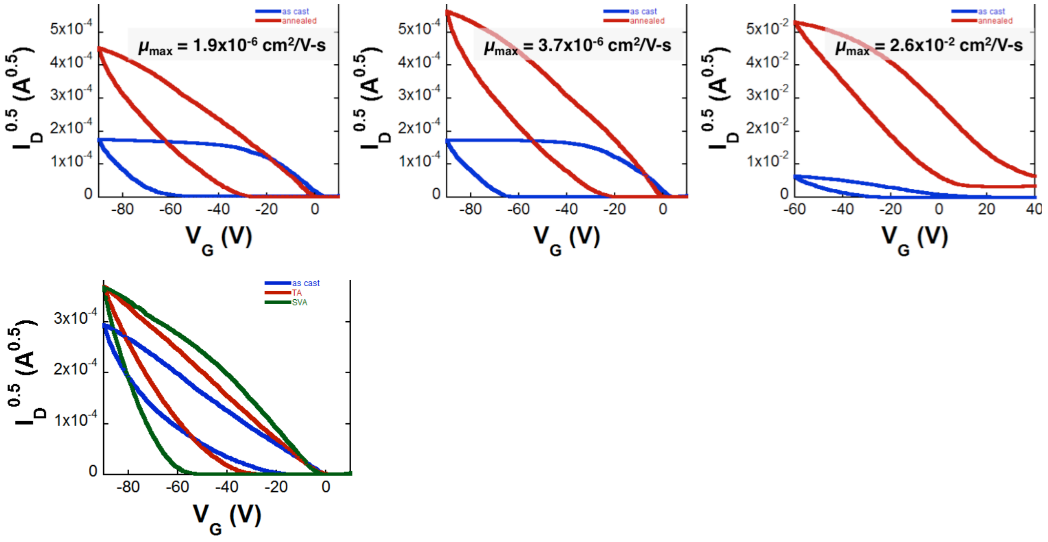

Fig. S8 Transfer curves of isomers **3a**, **3b**, **3c** (top from left to right), and the mixture (bottom). Blue: as-cast, red: thermally annealed, green: solvent-vapor annealed.

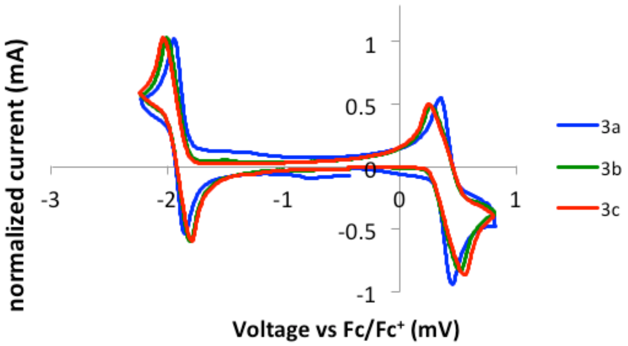

Fig. S9 Cyclic voltammetry measurements for isomers (**3a**, **3b**, **3c**) in 0.2 M solution of Bu_4 NPF_6 in dichloromethane at room temperature vs. (Fc/ Fc+) with Ag/AgCl as the reference electrode.

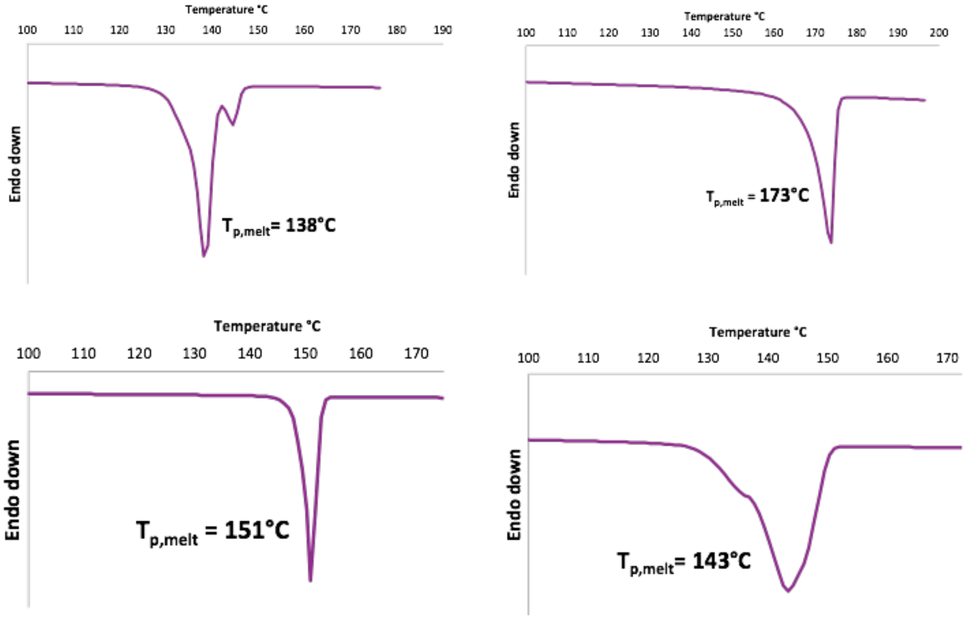

Fig. S10 Differential scanning calorimetry (DSC) spectra for isomers **3a** (top left), **3b** (top right), **3c** (bottom left), and the mixture of **3a**, **3b**, and **3c** (bottom right).

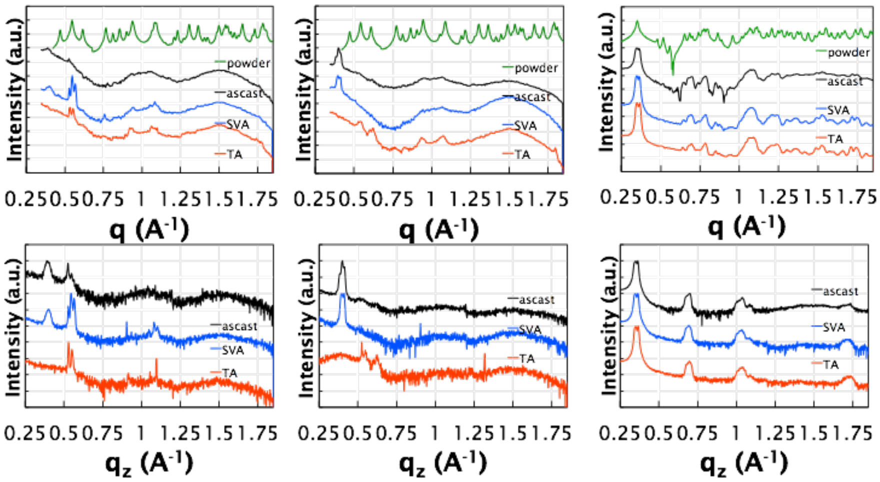

Fig. S11 Intensity vs. q (top), and intensity vs. q_z taken at $q_{xy} = 0$ Å^{-1} (bottom), for isomers **3a** (left), **3b** (middle), and **3c** (right).

Pair interaction energy decomposition analysis

The transformations used in recreating the crystal structure geometries are shown in Table S1. In each case, the x-axis lies along the long molecular axis, the y-axis along the short axis and the z-axis perpendicular to the π-system. In the case of the *anti* isomer, mirroring in the y-axis before transformation allowed modeling of disorder. The center of rotation was taken as the middle of the central acene ring, and translation was performed last of all.

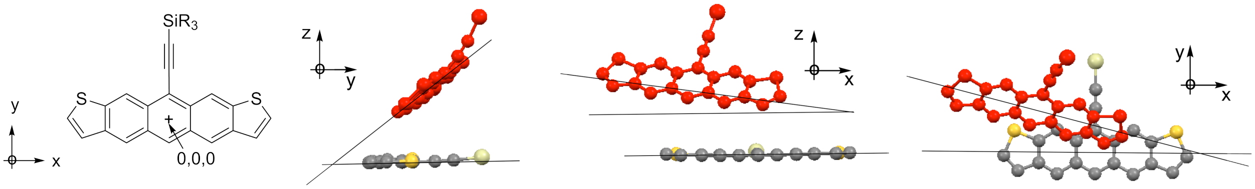

Table S1 Geometric transformations to recreate molecular pairs from crystal structures of **3a** and **3c**. Rotations are in degrees in a clockwise direction and translations are in Angstroms.

Contact	Rotation x-axis	Rotation y-axis	Rotation z-axis	Translation (x, y, z)
A-Pi	0	0	180	1.17, 0.57, -3.39
C-Pi	0	0	180	-3.56, 0.93, -3.45
C-1	43	13	7	-4.16, 2.57, 4.71
C-2	43	13	187	-4.24, -3.42, 3.07
C-3	0	0	180	1.46, -4.98, 2.53

The data from the PIEDA calculations is presented below. ES = electrostatic, EX = exchange, CT = charge transfer, DIS = dispersion and TE = total energy for the interaction depicted. All values are in kcal/mol.

Pair interaction energy decomposition analysis using isomer 3a

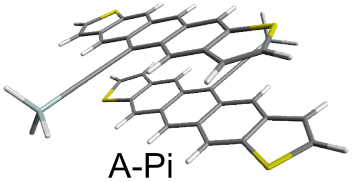

A-Pi

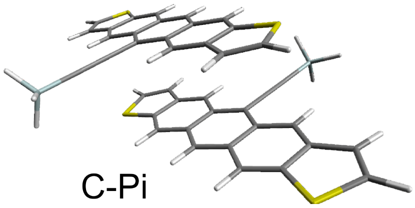

C-Pi

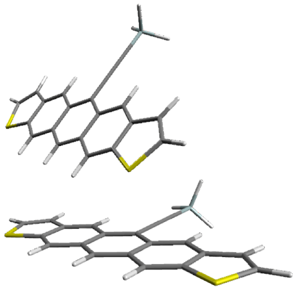

C-1

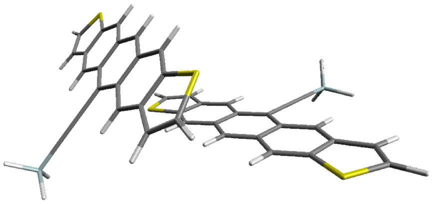

C-2

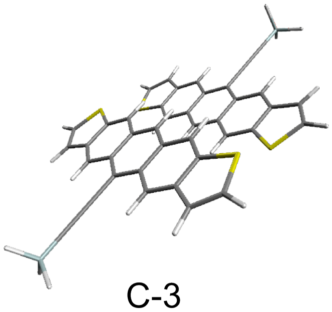

C-3

3a

	ES	EX	CT	DIS	TE
A-Pi	-10.61	29.37	-6.84	-49.57	-37.65
C-Pi	-3.77	12.21	-3.50	-31.82	-26.88
C-1	-7.55	17.07	-3.02	-20.31	-13.81
C-2	-2.42	5.45	-1.57	-14.00	-12.53
C-3	-8.32	15.98	-3.16	-19.66	-15.17

Pair interaction energy decomposition analysis using isomer 3b

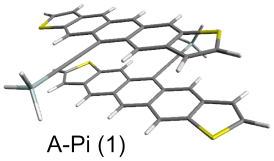
A-Pi (1)

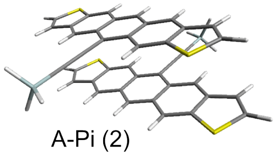
A-Pi (2)

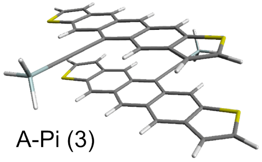
A-Pi (3)

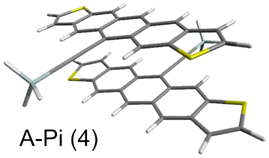
A-Pi (4)

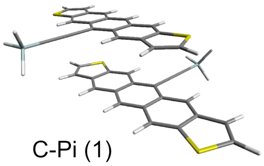
C-Pi (1)

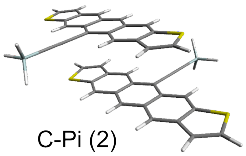
C-Pi (2)

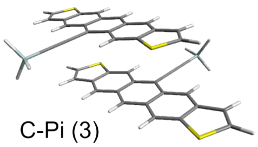
C-Pi (3)

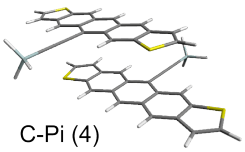
C-Pi (4)

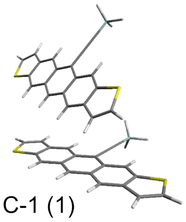
C-1 (1)

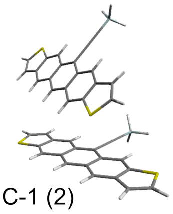
C-1 (2)

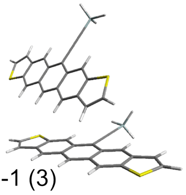
C-1 (3)

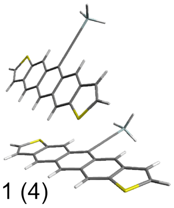
C-1 (4)

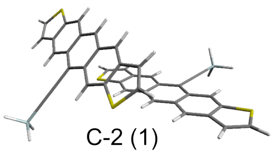
C-2 (1)

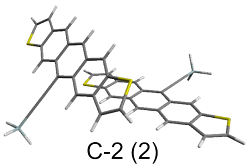
C-2 (2)

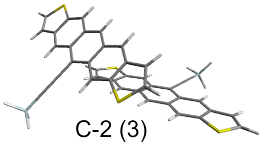
C-2 (3)

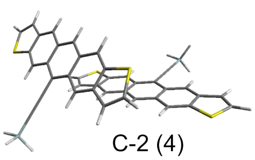
C-2 (4)

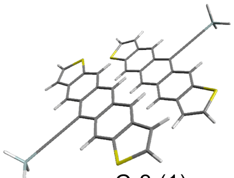
C-3 (1)

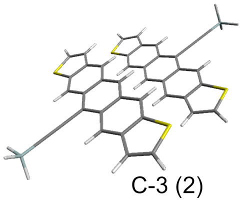
C-3 (2)

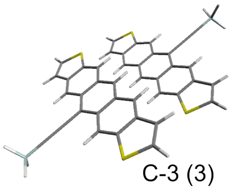
C-3 (3)

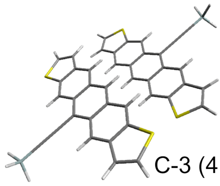
C-3 (4)

3b

		ES	EX	CT	DIS	TE
A-Pi	1	-9.95	29.22	-6.40	-48.40	-35.53
	2	-9.48	30.71	-6.50	-48.82	-34.09
	3	-9.47	28.84	-6.37	-48.14	-35.14
	4	-9.97	29.24	-6.41	-48.43	-35.56
	Ave	-9.72	29.50	-6.42	-48.45	-35.08
C-Pi	1	-6.01	17.99	-4.30	-36.79	-29.11
	2	-5.74	16.71	-4.29	-36.25	-29.57
	3	-5.99	19.20	-4.27	-37.28	-28.33
	4	-5.98	17.95	-4.29	-36.74	-29.06
	Ave	-5.93	17.96	-4.28	-36.76	-29.02
C-1	1	-5.90	11.10	-2.55	-18.06	-15.42
	2	-7.36	16.77	-2.99	-20.19	-13.77
	3	-5.91	11.64	-2.69	-18.28	-15.23
	4	-7.38	17.35	-3.13	-20.41	-13.56
	Ave	-6.64	14.21	-2.84	-19.23	-14.49
C-2	1	-2.92	5.48	-1.71	-13.98	-13.13
	2	-2.39	5.51	-1.58	-14.05	-12.50
	3	-3.39	4.21	-1.61	-13.17	-13.95
	4	-2.92	4.23	-1.47	-13.24	-13.40
	Ave	-2.91	4.86	-1.59	-13.61	-13.24
C-3	1	-7.81	13.70	-2.79	-18.56	-15.45
	2	-7.78	11.95	-2.58	-17.86	-16.27
	3	-8.00	14.71	-2.83	-19.01	-15.12
	4	-7.78	13.64	-2.78	-18.53	-15.45
	Ave	-7.84	13.50	-2.74	-18.49	-15.57

Pair interaction energy decomposition analysis using isomer 3c

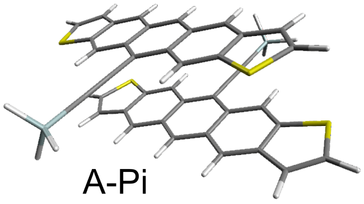
A-Pi

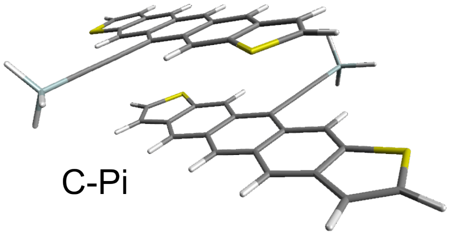
C-Pi

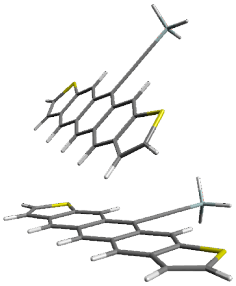
C-1

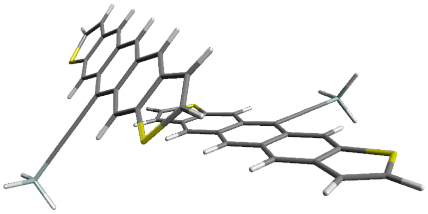
C-2

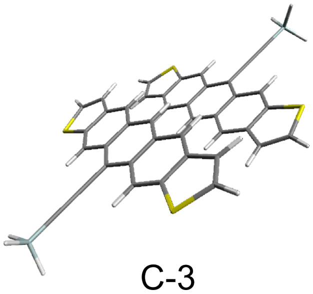
C-3

3c

	ES	EX	CT	DIS	TE
A-Pi	-10.38	31.81	-6.40	-49.23	-34.21
C-Pi	-6.53	19.27	-4.30	-37.29	-28.86
C-1	-5.80	11.72	-2.69	-18.33	-15.10
C-2	-3.42	4.27	-1.61	-13.19	-13.95
C-3	-7.35	11.61	-2.43	-17.56	-15.73

Electronic coupling calculations

The electron transfer module in NWChem was used to estimate charge transfer integrals rather than the HOMO splitting method, since the latter is affected by site energy differences in edge-to-face interactions. Using two molecules from the X-ray structure as geometries, the molecular orbitals of both molecules in neutral and radical cation electronic configurations were calculated independently, and then projected onto the dimer geometry in two pairs: neutral-radical cation and radical cation-neutral respectively, with no further optimization (i.e. localized orbitals on each molecule). The electron transfer module was then run, monitoring the reaction of transferring the charge from molecule 2 to molecule 1. This type of calculation is currently limited to Hartree-Fock methods in version 6.5 of NWChem.

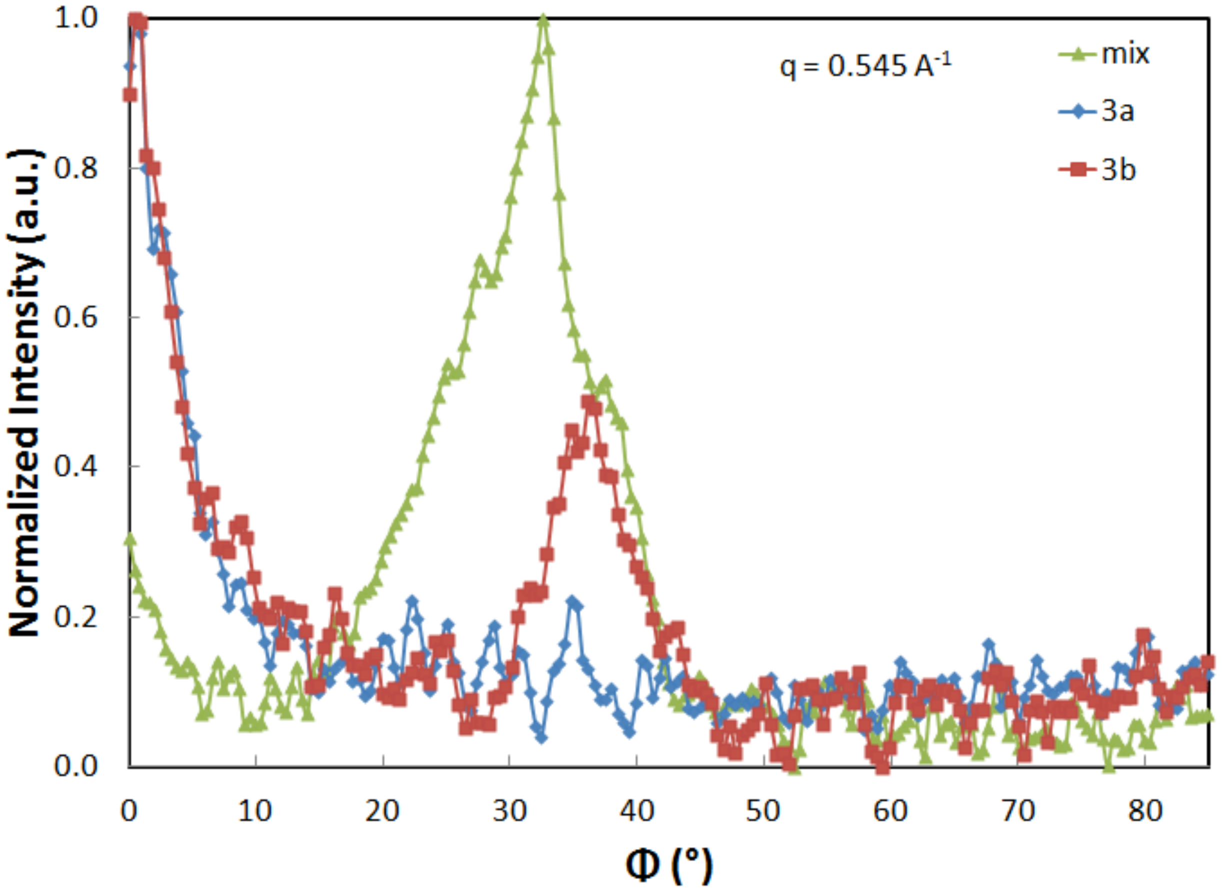

Fig. S12 Intensity of the (002) reflection vs. azimuthal angle of the mixture (**3a**+**3b**+**3c**), pure **3a**, and pure **3b** in thin films. To correlate the differences in mobility observed in Fig. 6 with changes in crystallite orientation, the data for **3a** and **3b** is extracted from the diffraction patterns of the thermally annealed films in Fig. 5, while the data for the mixture is extracted from the diffraction pattern of the solvent-vapor annealed film in Fig. 5.

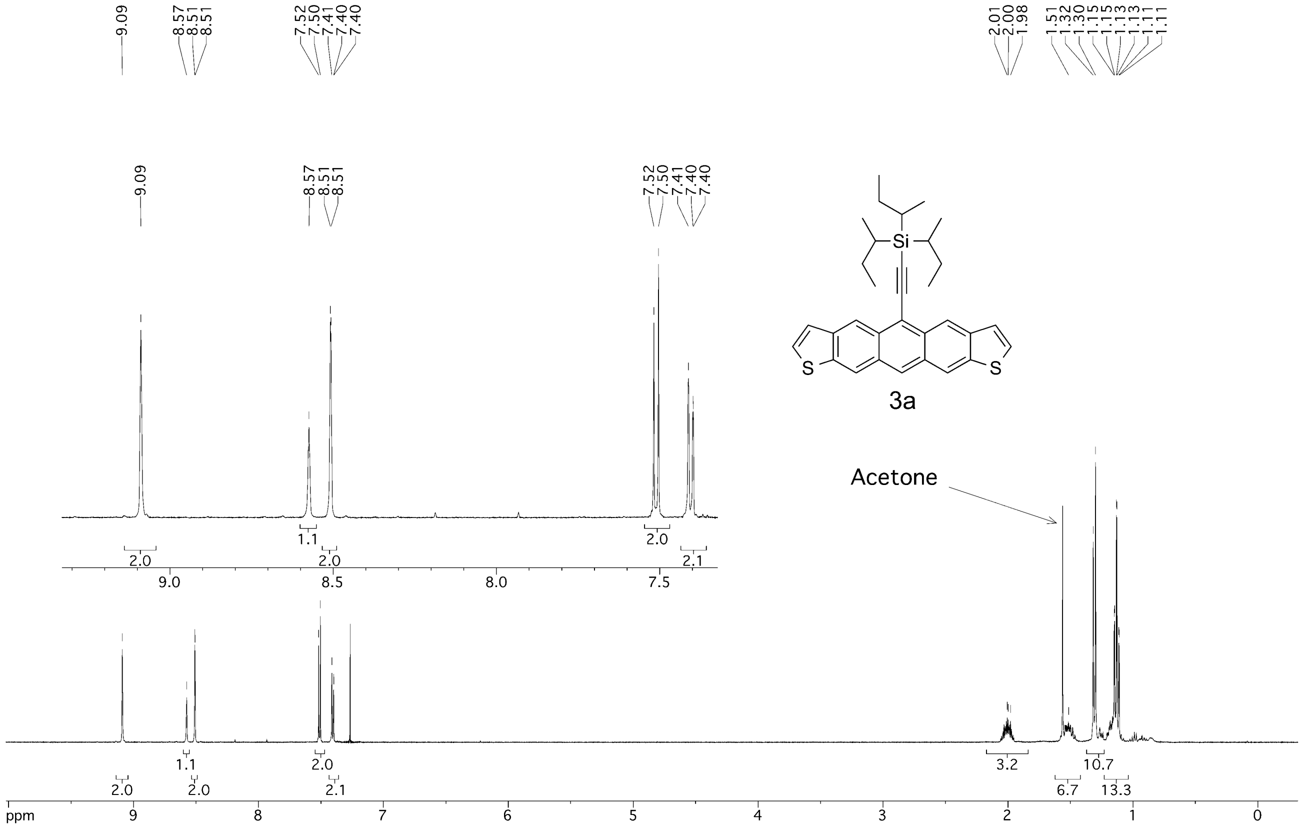

Fig. S13 ^{1}H NMR (400 MHz) of **3a** in $CDCl_3$.

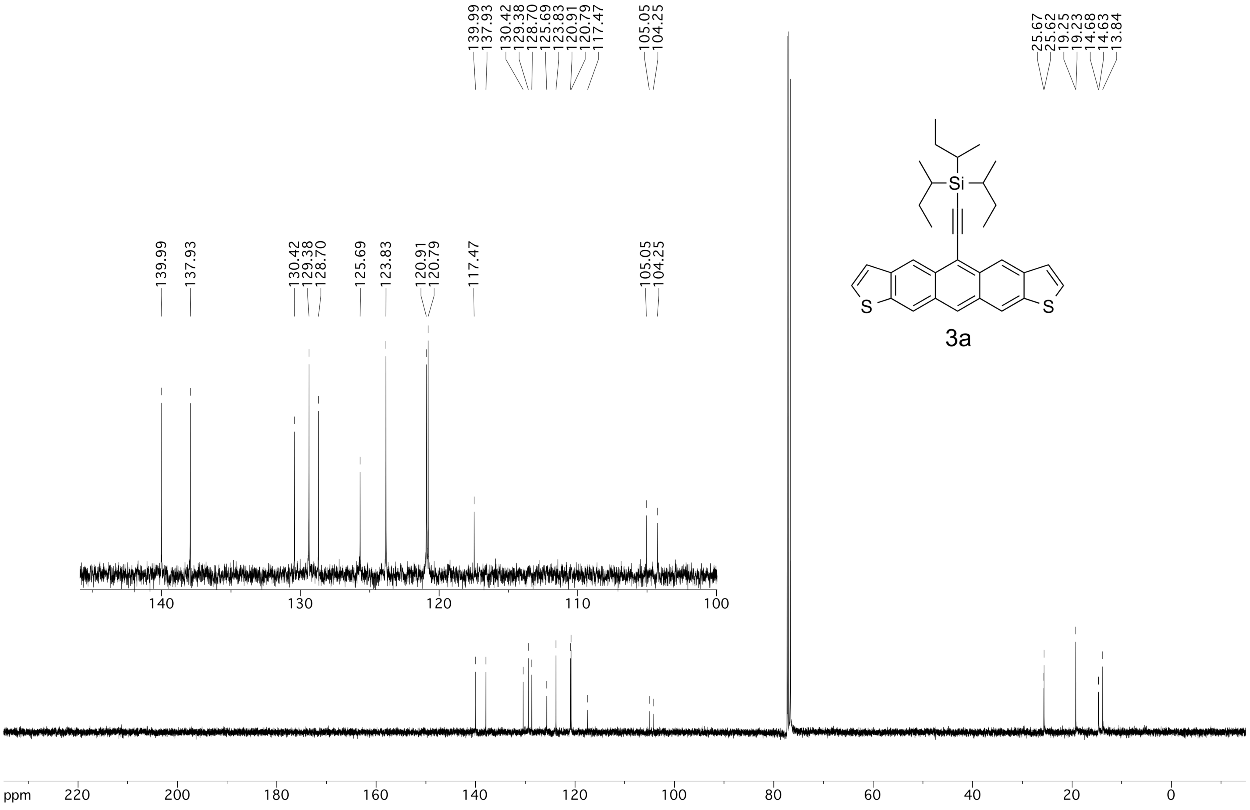

Fig. S14 ^{13}C NMR (100 MHz) of **3a** in CDCl$_3$.

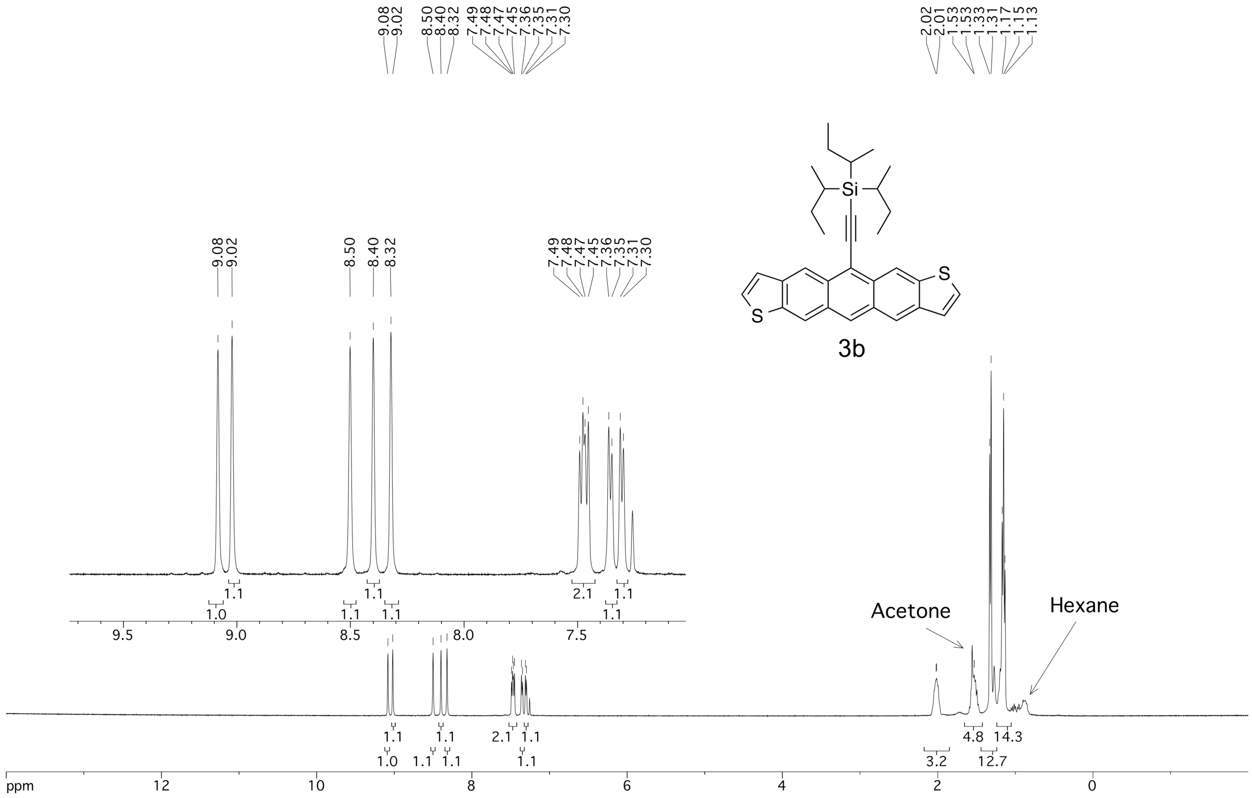

Fig. S15 ^{1}H NMR (400 MHz) of **3b** in $CDCl_3$

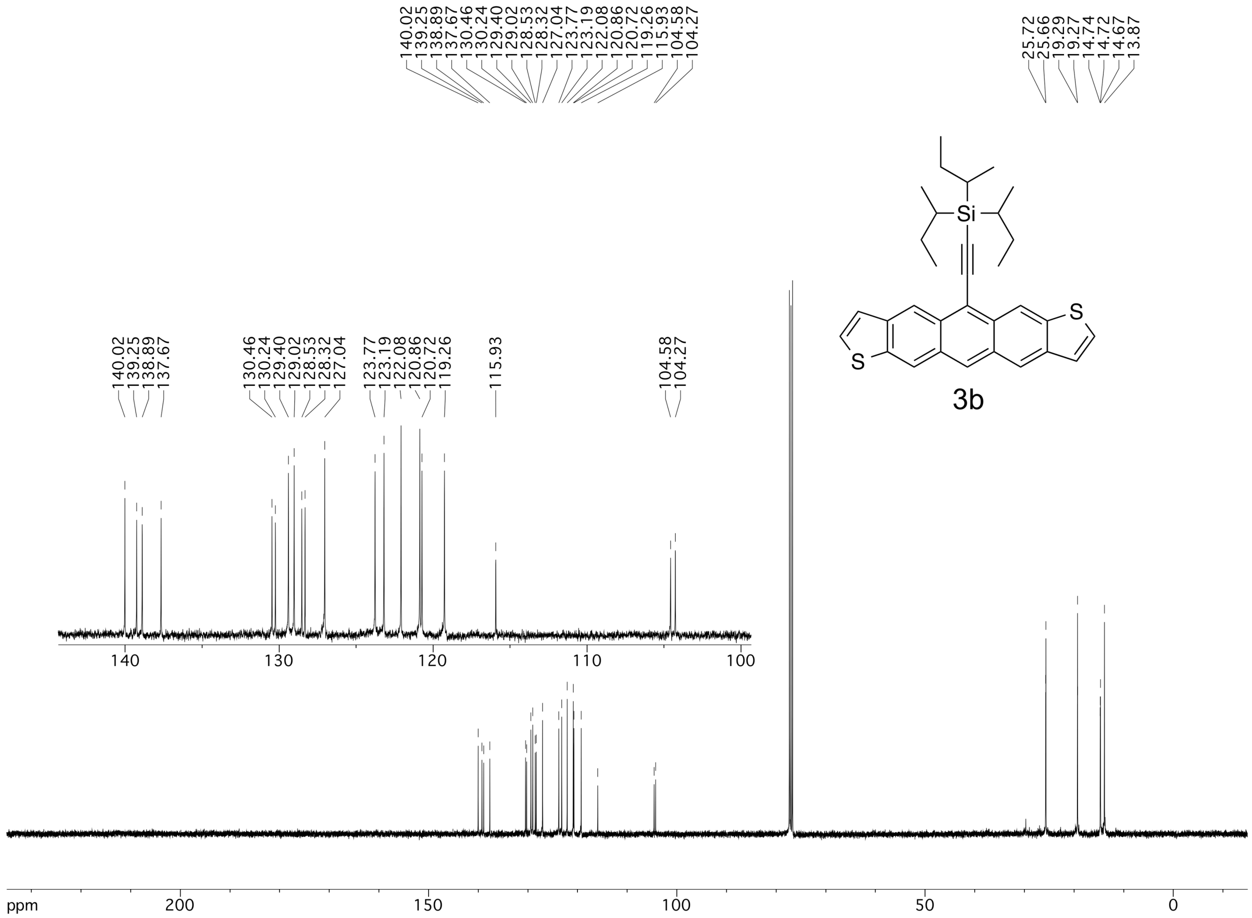

Fig. S16 ^{13}C NMR (100 MHz) of **3b** in $CDCl_3$.

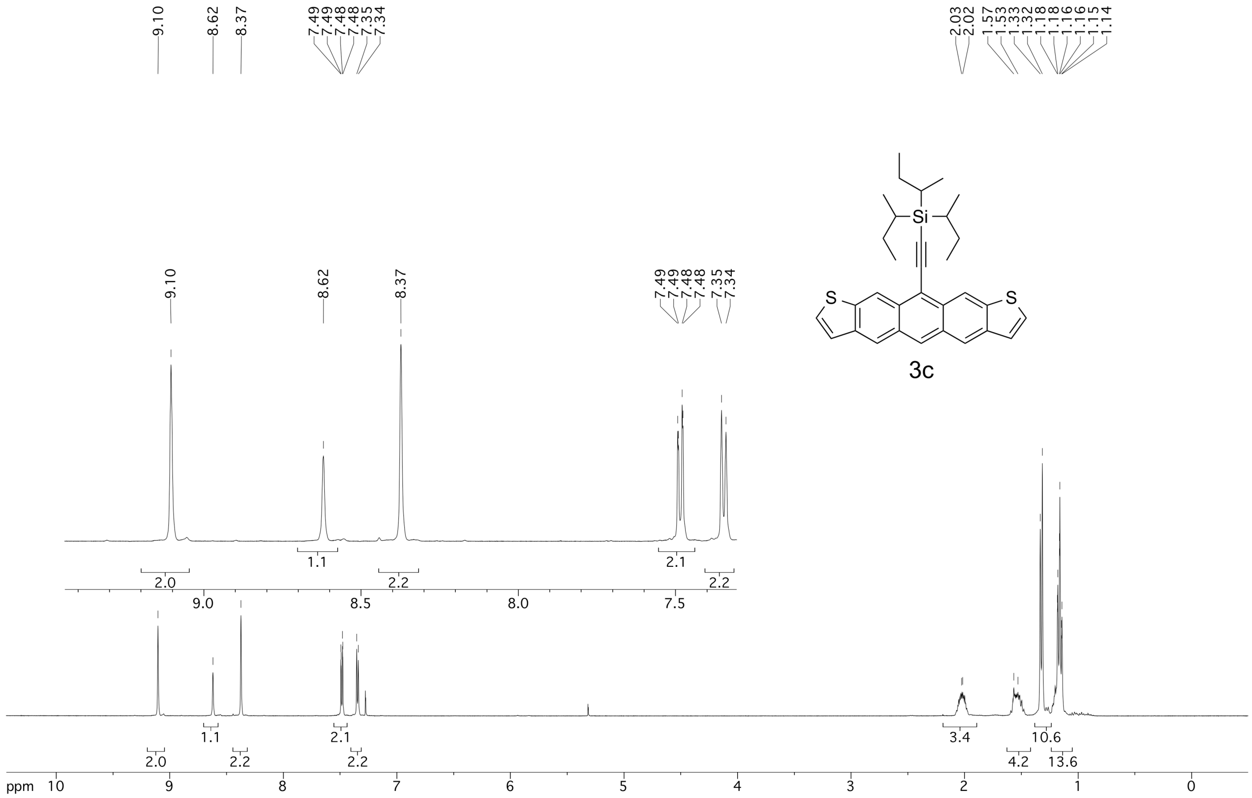

Fig. S17 ^{1}H NMR (400 MHz) of **3c** in $CDCl_3$.

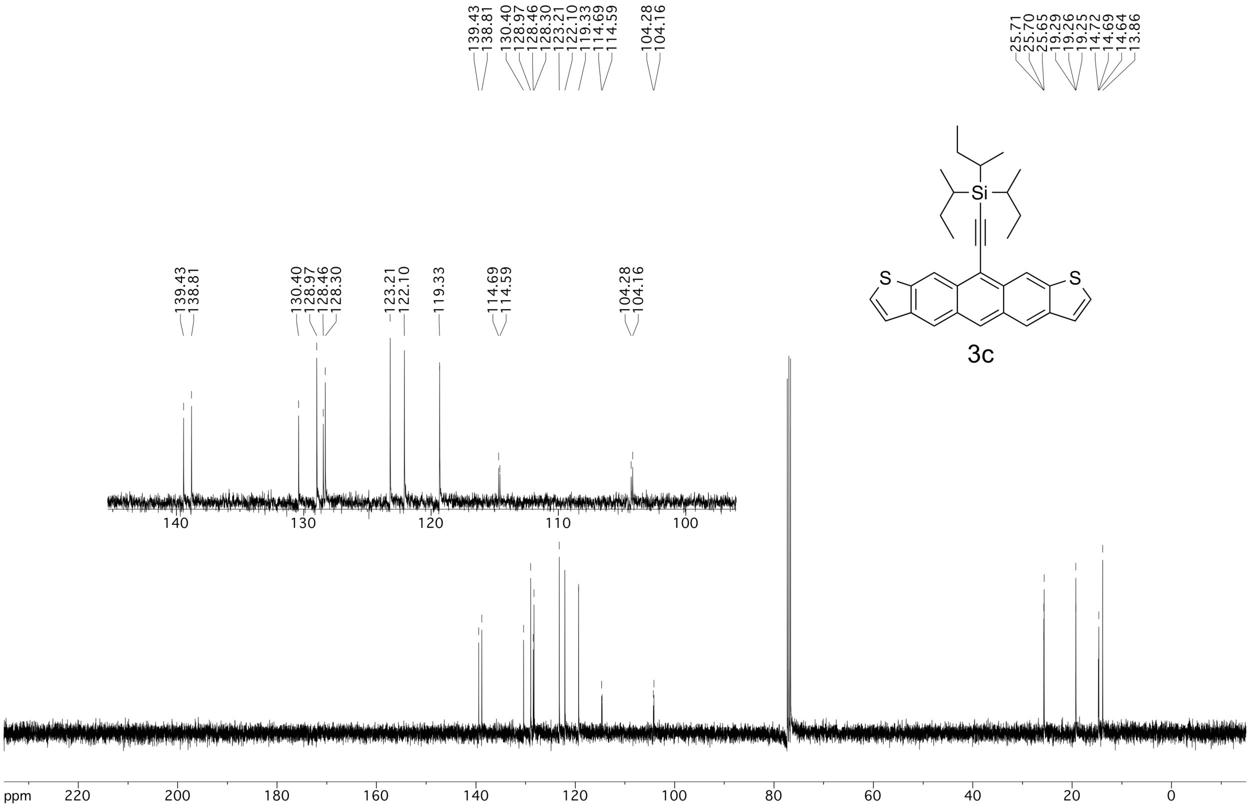

Fig. S17 ^{13}C NMR (100 MHz) of **3c** in $CDCl_3$.